IEEE Access
Multidisciplinary | Rapid Review | Open Access Journal

Received February 27, 2021, accepted March 11, 2021, date of publication March 23, 2021, date of current version March 31, 2021.

*Digital Object Identifier 10.1109/ACCESS.2021.3068085*

# Sensorless Simplified Finite Control Set Model Predictive Control of SynRM Using Finite Position Set Algorithm

**BEHNAM NIKMARAM[1], S. ALIREZA DAVARI[1], (Senior Member, IEEE), PEYMAN NADERI[1], CRISTIAN GARCIA[2], (Member, IEEE), AND JOSE RODRIGUEZ[3], (Fellow, IEEE)**

[1]Electrical Engineering Department, Shahid Rajaee Teacher Training University, Tehran 16788-15811, Iran
[2]Electrical Engineering Department, Faculty of Engineering, Universidad de Talca, Curico 3340000, Chile
[3]Department of Engineering Science, Faculty of Engineering, Universidad Andrés Bello, Santiago 8370146, Chile

Corresponding author: S. Alireza Davari (davari@sru.ac.ir)

The work of Cristian Garcia and Jose Rodriguez was supported by the Agencia Nacional de Investigación y Desarrollo (ANID) through the Project under Grant FB0008, Grant ACT192013, Fondecyt 1210208, and Fondecyt 11180235.

**ABSTRACT** The sensorless application of predictive control in drive applications has been investigated for a decade. Finite control set model predictive control (FCS-MPC) is one of the easy and practical methods in the predictive category. Several methods have been investigated for the sensorless application of FCS-MPC. Since the sensitivity of the predictive method to the speed error is more than that of the classical control methods, sophisticated speed estimators should be used in this method. The model reference adaptive system (MRAS) has been the most successful estimator. The main problem of this estimator is tuning the coefficients in different operating points and the stability of the adaptive function. The finite position set technique is a very recent solution. In this method, the adaptive function is used as the cost function and the optimum rotor position is selected by minimizing that. However, the numerous iteration is a barrier for application to the predictive method. Also, the application of the method for the synchronous reluctance motor (SynRM) is a challenge because of the lack of the rotor model as the adaptive function. In this paper, the finite position technique is modified for the predictive application. The number of iterations is reduced by an optimization method based on sensitivity analysis. Also, a new and simple function is used as the adaptive error function in order to apply the method to the sensorless control of the SynRM. The proposed method is evaluated by simulation and experiment.

**INDEX TERMS** Motor drives, predictive control, synchronous reluctance motor, sensorless control.

## I. INTRODUCTION

Synchronous reluctance motor has recently received much attention from researchers. The ability of this motor for high-temperature applications and high efficiency of this motor, also high resistance against the centrifugal force are the reasons for this attention [1], [2].

On the other hand, model predictive control has been successfully applied to power electronics and drives applications in the recent decade [3], [4]. Better dynamics [5], [6] and smaller torque ripple [7] was the outcome of applying this method to different motors. One of the predictive methods used for control of the synchronous reluctance motor is the FCS-MPC method [8]. Despite advantages such as fast dynamic and easy implementation, [9], [10], a problem of this method is a high volume of computation because the prediction should be performed for all available switching states. To overcome this problem the simplified FCS-MPC was introduced in which the voltage-based cost function is applied [8], [11]. Also, the computations are reduced while the optimum dynamics and ripples were achieved in [7].

Control of the motor without the speed sensor is another application that researchers have paid much attention to it [12]. A few investigations that have focused on the sensorless simplified FCS-MPC method, are [13], [14]. These two works performed sensorless simplified FCS-MPC through a Luenberger observer for the induction motor. This method has problems, especially in the low-speed range. Considering

The associate editor coordinating the review of this manuscript and approving it for publication was Jinquan Xu.

the synchronous reluctance motor, the sensorless application of the simplified FCS-MPC method has not been addressed. The following is a summary of the sensorless applications method implemented on the synchronous reluctance motor.

There are different methods for sensorless control of SynRM for various ranges of speed in drive applications [15], [16]. Generally speaking, sensorless methods are divided into two main categories. The first category includes the techniques without signal injection [17], [18], and the second category uses high frequency signal injection [19], [20]. The signal injection method cannot be applied to the FCS-MPC because of the lack of the modulator which prevents injection of the high-frequency signal to the voltage of the inverter [21]. Therefore, it is not considered in the review of this paper.

A method in the first category is the observer-based method. Different observers have been employed and designed in sensorless predictive control. Model reference adaptive system (MRAS) is one of the most successful observers that is presented in [22]. This method is a model-based method and the flux or current error of the motor is used for estimating the position of the motor by means of a PI controller. This method has problems such as pure integration effects, tuning the PI controller parameters, and sensitivity in the low-speed region. The observer with sliding mode feedback gains is presented in [23]. In this method, the sensitivity to parameter variation is lower than conventional MRAS but the other problems of MRAS still persist. Furthermore, the application of an adaptive speed estimator is more difficult for the SynRM because of the lack of rotor winding. Usually, it is prevalent to use the stator model as the reference model and the rotor model as the adaptive model in two-winding machines [24]. Luenberger observer and Kalman filter are presented for better performance in the low range of the speeds [25]–[27]. But these methods are sensitive to the parameter variation and they need to accurately design their coefficient and they have high computation.

Another method that does not use observer but can be placed in the first category is the optimization-based position sensorless control method that is presented in [21]. In this method, the speed of the motor is calculated by transferring the model of the machine into an estimation reference frame. This method is suitable for all ranges of speed but it is very sensitive to parameter variation and it has a high computation. Also, this method is done for IPMSMs because it is dependent on the model of this motor. The convergence of this method is dependent on the magnetic flux term of this motor. Therefore, this method can't be converged for the synchronous reluctance motor.

Model predictive MRAS estimator [28] has shown stable performance in all ranges of speeds. This method improved the conventional MRAS method through an iteration-based algorithm. It doesn't need a PI controller for estimation of the rotor position. This method resolves problems of conventional MRAS and it doesn't need the signal injection for speed estimation in the low-speed ranges. This method has been investigated for the induction motor in field-oriented control method in [29], [30]. Because of the numerous iterations that are needed for this method, that is not applicable for FCS-MPC in real life which needs several predictions itself. Therefore, it is only applied to the field-oriented control method in both references. Also, application of the used error function for the SynRM is a new challenge because of the lack of rotor winding which results in the lack of rotor model as the adaptive model.

In this paper, a modified finite positioning algorithm and a new error function is used for the simplified FCS-MPC method for SynRM. The number of iterations is reduced by an optimization based on the sensitivity analysis. Thus, the method became applicable to the FCS-MPC. On the other hand, a simplified predictive method is used in order to eliminate several predictions of the torque and flux. Furthermore, the error function is formed by a flux-based error. The flux is estimated in the stationary frame as the reference model and in the rotating frame as the adaptive one. Its transformed form to the stationary frame is used in the error function. The rotor angle which is used in the transformation is discretized and optimized by the proposed error function. The proposed error function is analytically proved. By this error function, the method is easily applicable for the SynRM.

## II. MATHEMATICAL MODEL OF SynRM

The dynamic model of SynRM is only related to the stator since there is no rotor winding in this motor. The mathematical model of SynRM in rotor oriented rotating reference frame ($dq$) is as follows [20]:

$$v_d = r_s i_d + \frac{d\lambda_d}{dt} + \omega\lambda_q \tag{1a}$$

$$v_q = r_s i_q + \frac{d\lambda_q}{dt} - \omega\lambda_d \tag{1b}$$

where $v_d$ and $v_q$ are the stator voltages, $i_d$ and $i_q$ are the stator currents, $\lambda_d$ and $\lambda_q$ are the flux linkages, and $\omega$ is the electrical motor speed.

The torque can be expressed by the following equation.

$$T = \frac{3}{2} p \lambda_e i_q \tag{2a}$$

$$\lambda_e = \left(L_d - L_q\right) i_d \tag{2b}$$

where $\lambda_e$ is the defined active flux.

## III. SIMPLIFIED FCS-MPC FOR SynRM

Generally in the finite control set model predictive method, the discrete nature of the inverter is considered in the control algorithm. All of the possible voltage vectors of the inverter are imported and tested into the dynamic model of the motor and the future behavior of the motor is predicted for each of them. In order to avoid tuning weighting factor in the classic FCS-MPC [23], the simplified FCS-MPC has been introduced instead of the classic FCS-MPC [11]. In this method, the reference voltage is predicted based on the references of

the torque and the flux, and the following cost function is used instead of the conventional cost function which consists of the torque and flux errors.

$$C_n = \left|\vec{v}_{k+1_n} - \vec{v}^*_{k+1_n}\right| \tag{3}$$

where $n$ is the number of the voltage vector, $C$ is the cost function. Subscript $k+1$ shows the next sampling interval and superscript $*$ shows the reference value.

By this method, the seven voltage vectors of the inverter are directly used in the cost function. The reference voltage vector should be predicted in every sampling interval due to the torque and flux references.

To do so, the rotor-oriented frame is used. Based on (2), the future current components should be equal to the following references.

$$i^*_{d_{k+1}} = \lambda^*_e / \left(L_d - L_q\right) \tag{4a}$$

$$i^*_{q_{k+1}} = T^* / \frac{3}{2} p \lambda^*_e \tag{4b}$$

where $\lambda^*_e$ is the reference of the active flux.

Now, by using (1), and (4) the voltage reference in the rotor-oriented frame is predicted.

$$v^*_{d_{k+1}} = \frac{L_d(i^*_{d_{k+1}} - i_{d_k})}{t_s} + r_s i_{d_k} + \omega L_q i_{q_k} \tag{5a}$$

$$v^*_{q_{k+1}} = \frac{L_q(i^*_{q_{k+1}} - i_{q_k})}{t_s} + r_s i_{q_k} - \omega L_d i_{d_k} \tag{5b}$$

The predicted voltage should be transformed to the stationary frame to be used in the cost function (3).

$$\vec{v}^*_{k+1} = \left(v^*_{d_{k+1}} + j v^*_{q_{k+1}}\right) e^{j\omega t} \tag{6}$$

where $j = \sqrt{-1}$.

Therefore, though the simplified FCS-MPC eliminates the weighting factor it is harder to be implemented without the encoder because the correct phase angle of the reference voltage is completely dependent on the angular speed based on (6).

## IV. SENSORLESS SIMPLIFIED FCS-MPC

A speed or position sensor is needed in order to implement the simplified FCS-MPC method which will be used in (5) an (6). Thus, the estimated speed will influence the prediction model and the direct and quadrant current control consequently in the sensorless application. The finite position set algorithm is a recent, accurate, and robust algorithm [29], [30]. The application of this technique for predictive control is a challenge because of the numerous iterations. On the other hand, using it for control of the synchronous reluctance motor is another challenge. These two issues are addressed in this research.

### A. FINITE POSITION SET ALGORITHM

The finite position set model predictive algorithm is a new technique that has been proposed in order to use the phase locked loop (PLL) in a finite solution form [29], [30]. An idea similar to the idea of FCS-MPC is used in this technique. Finite positions are examined in the error cost function and the position that minimizes the cost function will be chosen. Therefore, a certain value for the position error is always part of the accepted solution. In the method proposed in [29], [30], Algorithm 1 is used in order to define the finite set of positions.

**Algorithm 1** Finite Positioning in [30]

**for** $(i_1 = 0, \cdots, 7)$ **do**
  $\Delta\theta_{i_1} = (\pi/4)2^{-i_1}$
  **for** $(i_2 = 0, \cdots, 7)$ **do**
    $\theta_{i_1,i_2} = \theta_{opt_{i_1}} + (i_2 - 4)\Delta\theta_{i_1}$
    estimate $\hat{v}_{s_{d_{i_2}}}$ by using $\theta_{i_1,i_2}$ the motor model
    calculate $e_{\theta_{i_2}} = |v_{s_d} - \hat{v}_{s_{d_{i_2}}}|$
  **end for**
  select $\theta_{opt_{i_1}}$ based on **min** $e_{\theta_{i_2}}|_{(i_2=0,\cdots,7)}$
**end for**
$\hat{\theta} = \theta_{opt_7}$

In this algorithm, the complete space is divided by 8 and the closest position is chosen based on the minimum error function. Afterwards, the accuracy is doubled, i.e., the step is divided by 2, and the 8 positions around the selected one are checked by the error function. This procedure is repeated 8 times. The accuracy is doubled each time. Thus, the accuracy of the final solution will be $\pi/512$.

The error function which is used in [30] is based on the voltage error.

$$e_\theta = \left|v_{s_d} - \hat{v}_{s_d}\right| \tag{7}$$

where $v_{s_d}$ is the direct component of the measured voltage of the stator and $\hat{v}_{s_d}$ is that of the estimated voltage by the machine model.

There are two problems with this method:

- The error function should be calculated 64 times for each sampling interval.
- The error function which is used as the cost function is based on accurate stator voltage.

In this research, these problems are amended by the following improvements.

### B. OPTIMIZING THE ACCURACY

The expense of the high accuracy is higher processing power. Calculating the cost function 64 times needs a high amount of process. However, this accuracy will not really be necessary for FCS-MPC if the finite number of the voltage vectors are considered. Namely, there would be torque ripples because of using an inverter with a limited number of switching states. The sensitivity of the $q$-axis current to the rotor position error is studied in order to find an optimum accuracy because this component of the current is related to the torque.

$$S_\theta^{i^*_{q_{k+1}}} = A_1 \sin\theta + A_2 \cos\theta \tag{8a}$$

$$A_1 = -i_\beta - \frac{t_s}{L_q}\left(v_\beta - r_s i_\beta - \frac{d\theta}{dt} L_d i_\alpha\right) \tag{8b}$$

$$A_2 = -i_\alpha + \frac{t_s}{L_q}\left(-v_\alpha + r_s i_\alpha - \frac{d\theta}{dt} L_d i_\beta\right) \quad (8c)$$

where $S_\theta^{i^*_{q_{k+1}}}$ is the sensitivity of $i^*_{q_{k+1}}$ to the rotor position.

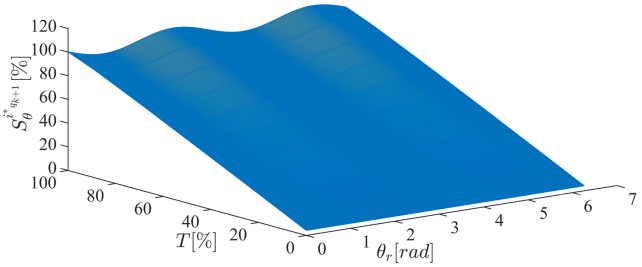


**FIGURE 1.** Sensitivity of $i^*_{d_{k+1}}$ to the rotor position.

Fig. 1 shows the sensitivity of the $q$-axis component of the current to the rotor position in different torques. Based on this investigation, the maximum sensitivity is 106.1%. On the other hand, if 5% current ripple is considered as the acceptable ripple, the maximum accepted error for the position angle can be found by the following equation. Note that these limits are set as the samples to show how accurate will be the final results. In fact, they could be the outcome of a compromisation between the switching frequency and accuracy. Also, they can be manipulated if the performance of the system is not satisfactory at the end.

$$\Delta\theta = \frac{\Delta i^*_{q_{k+1}}}{S_\theta^{i^*_{q_{k+1}}}} \quad (9a)$$

$$\Delta\theta_{\max} = 0.05/1.061 = 0.0471 \quad (9b)$$

where $\Delta\theta$ is the position error and $\Delta i^*_{q_{k+1}}$ is the current ripple.

Thus, by selecting $i_1 = 0, 1, \cdots, 6$ and $i_2 = 0, 1, 2$, the final $\Delta\theta$ is equal to $(2\pi/3)2^{-6} = \pi/96 = 0.0327$ which is smaller than $\Delta\theta_{\max}$.

**Algorithm 2** Proposed Finite Positioning

estimate the reference flux ($\vec{\lambda}_{\alpha\beta_{ref}}$) by (10)
**for** ($i_1 = 0, \cdots, 6$) **do**
  $\Delta\theta_{i_1} = (2\pi/3)2^{-i_1}$
  **for** ($i_2 = 0, 1, 2$) **do**
    $\theta_{i_1,i_2} = \theta_{opt_{i_1}} + (i_2 - 1)\Delta\theta_{i_1}$
    estimate the adaptive flux ($\vec{\lambda}_{\alpha\beta_{ad_{i_2}}}$) by (11) and (12)
    calculate $e_{\theta_{i_2}} = \left|\lambda_{\alpha_{ref}}\lambda_{\beta_{ad_{i_2}}} - \lambda_{\beta_{ref}}\lambda_{\alpha_{ad_{i_2}}}\right|$
  **end for**
  select $\theta_{opt_{i_1}}$ based on **min** $e_{\theta_{i_2}}|_{(i_2=0,1,2)}$
**end for**
$\hat{\theta} = \theta_{opt_6}$

Algorithm 2 shows the proposed optimized finite positioning. The number of iterations in each control interval is reduced to 24 by the proposed method.

Fig. 2 shows an example of the finite positions of the proposed method for four iterations. In the first iteration ($i_1 = 0$),

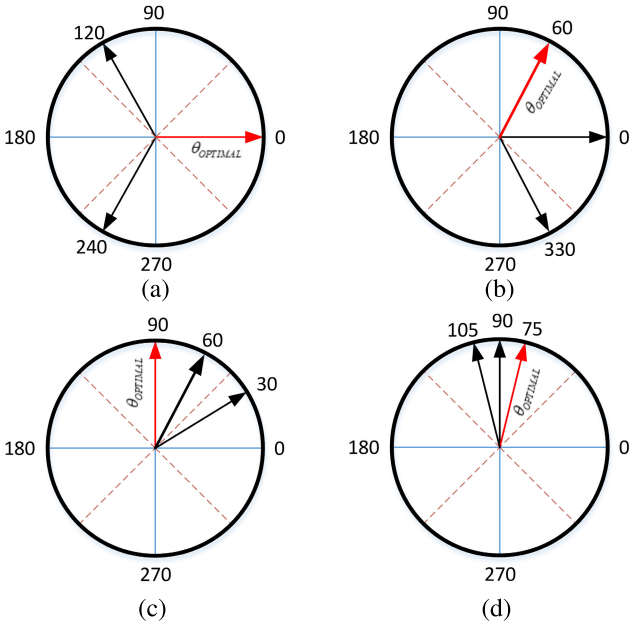


**FIGURE 2.** Finite Positions of the proposed method for (a) $i_1 = 0$ ($\Delta\theta = 2\pi/3$) (b) $i_1 = 1$ ($\Delta\theta = \pi/3$) (c) $i_1 = 2$ ($\Delta\theta = \pi/6$) (d) $i_1 = 3$ ($\Delta\theta = \pi/12$).

the complete $2\pi$ rad is covered by examining three options, i.e., $\theta_{0,1} = -2\pi/3, \theta_{0,2} = 0, \theta_{0,3} = 2\pi/3$. The position which results in the minimum error function is selected as the optimum of this iteration, e.g., $\theta_{opt_0} = 0$. For the second iteration ($i_1 = 1$), the last selected position and the positions which are located at $\pm\pi/3$ before and after that are the new set of the finite positions. This algorithm is repeated until $i_1 = 6$.

In this research, a new error function is proposed and used in this algorithm which will be explained in the following subsection.

### C. PROPOSED ERROR FUNCTION

The error function (7) consists of the voltage error which needs voltage measurement for accurate performance. A new error function is proposed in this paper.

The error function of MRAS systems has been widely investigated for classic methods for the induction motor. Usually, the stator and rotor models are used as the reference and the adaptive systems, respectively [28]. However, this method is not possible for SynRM motor because of the lack of rotor winding. A flux-based function is proposed in this research.

The motor model in the stationary frame is used as the reference model.

$$\vec{\lambda}_{\alpha\beta_{ref}} = \int (\vec{v}_{\alpha\beta} - r_s\vec{i}_{\alpha\beta})dt \quad (10)$$

where $\vec{\lambda}_{\alpha\beta_{ref}} = \lambda_{\alpha_{ref}} + j\lambda_{\beta_{ref}}$ is the reference estimated flux in MRAS method, and $\vec{v}_{\alpha\beta} = v_\alpha + jv_\beta$, and $\vec{i}_{\alpha\beta} = i_\alpha + ji_\beta$.

The rotating frame model is used as the adaptive system.

$$\vec{\lambda}_{dq_{ad}} = \int (\vec{v}_{dq} - r_s\vec{i}_{dq} + j\omega\vec{\lambda}_{dq_{ad}})dt \quad (11)$$

Note that the forward Euler discretization method is used in order to avoid the algebraic loop. The returned form of the $\vec{\lambda}_{dq_{ad}}$ to the stationary frame is used as the adaptive estimated flux.

$$\vec{\lambda}_{\alpha\beta_{ad}} = \vec{\lambda}_{dq_{ad}} e^{j\omega t} \tag{12}$$

Thus, the proposed error function can be defined as below:

$$e_\theta = \left|\lambda_{\alpha_{ref}} \lambda_{\beta_{ad}} - \lambda_{\beta_{ref}} \lambda_{\alpha_{ad}}\right| \tag{13}$$

*Proof:* The following inaccurate model in the rotating frame can be found out based on (1).

$$\frac{d\hat{\vec{\lambda}}}{dt} = \frac{d(\vec{\lambda}+\Delta\vec{\lambda})}{dt} = \vec{v} - r_s\vec{i} + j(\omega_0+\Delta\omega)(\vec{\lambda}+\Delta\vec{\lambda}) \tag{14}$$

where $\omega_0$ is the accurate angular speed, and $\Delta\omega$ is the error of the speed. Also, $\hat{\vec{\lambda}}$ is the inaccurate flux, $\vec{\lambda}$ is the accurate flux, and $\Delta\vec{\lambda}$ is the error of the flux.

By subtracting (14) by (1), the error model can be achieved.

$$\frac{d\Delta\lambda_d}{dt} = \Delta\omega\left(\lambda_q + \Delta\lambda_q\right) + \omega_0\Delta\lambda_q \tag{15a}$$

$$\frac{d\Delta\lambda_q}{dt} = -\Delta\omega\left(\lambda_d + \Delta\lambda_d\right) - \omega_0\Delta\lambda_d \tag{15b}$$

By replacing $\Delta\omega = d\Delta\theta/dt$ and $\omega_0 = d\theta_0/dt$ in (15), the following is gotten.

$$\frac{d\Delta\lambda_d}{dt} = (d\Delta\theta/dt)\left(\lambda_q + \Delta\lambda_q\right) + (d\theta_0/dt)\Delta\lambda_q \tag{16a}$$

$$\frac{d\Delta\lambda_q}{dt} = -(d\Delta\theta/dt)\left(\lambda_d + \Delta\lambda_d\right) - (d\theta_0/dt)\Delta\lambda_d \tag{16b}$$

Now, a proper Lyapunov function is defined.

$$V = \frac{1}{2}(\Delta\lambda_d)^2 + \frac{1}{2}(\Delta\lambda_q)^2 + \frac{1}{2}(\Delta\theta)^2 \tag{17}$$

The derivative of this function by using (16) is as follows:

$$\begin{aligned}\frac{dV}{dt} = &\left[(d\Delta\theta/dt)\left(\lambda_q + \Delta\lambda_q\right) + (d\theta_0/dt)\Delta\lambda_q\right]\Delta\lambda_d \\ &- \left[(d\Delta\theta/dt)\left(\lambda_d + \Delta\lambda_d\right) + (d\theta_0/dt)\Delta\lambda_d\right]\Delta\lambda_q \\ &+ (d\Delta\theta/dt)\Delta\theta\end{aligned} \tag{18}$$

The simplified form of (18) is (19).

$$\frac{dV}{dt} = (d\Delta\theta/dt)(\lambda_q\Delta\lambda_d - \lambda_d\Delta\lambda_q) + \Delta\theta(d\Delta\theta/dt) \tag{19}$$

By considering that $\Delta\lambda_d = \lambda_d - \hat{\lambda}_d$ and $\Delta\lambda_q = \lambda_q - \hat{\lambda}_q$, the following equation will be derived:

$$\frac{dV}{dt} = (d\Delta\theta/dt)(\lambda_d\hat{\lambda}_q - \lambda_q\hat{\lambda}_d) + \Delta\theta(d\Delta\theta/dt). \tag{20}$$

The derivative of the Lyapunov function should be negative in order to have an stable observer. Since $\Delta\theta$ is reduced every iteration in Algorithm 2, $d\Delta\theta/dt$ is a negative value. Thus, if the method is converged, the term that multiplied by that should be positive.

$$(\lambda_d\hat{\lambda}_q - \lambda_q\hat{\lambda}_d) + \Delta\theta < 0 \tag{21}$$

It shows that the maximum value of the position error ($\Delta\theta$) is $\left|\lambda_d\hat{\lambda}_q - \lambda_q\hat{\lambda}_d\right|$. Therefore, minimization of this error function is a stable criterion for the convergence. The achieved cost function is the exterior product and it would be correct in the stationary frame as (13).

### D. COMPLETE PROPOSED SENSORLESS SIMPLIFIED FCS-MPC

The complete block diagram of the proposed method is depicted in Fig. 3. The position of the rotor is estimated by the proposed algorithm finite position set block and the result is given to the simplified FCS-MPC block.

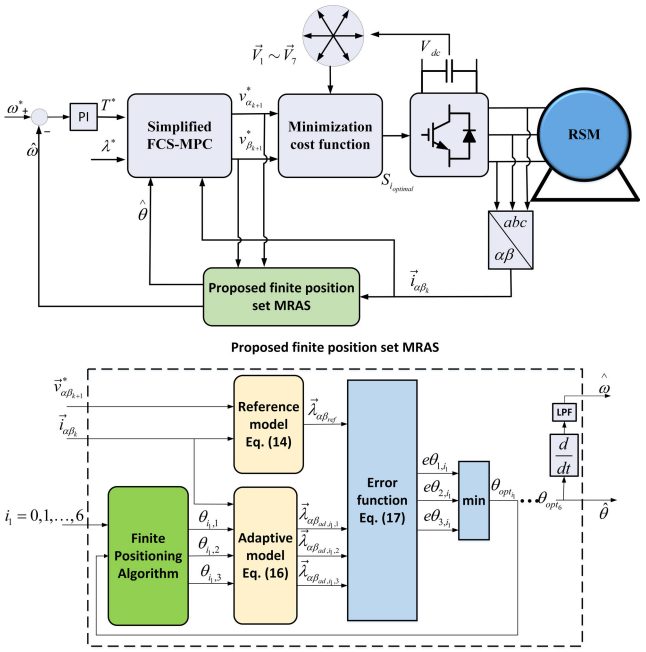


**FIGURE 3.** Block diagram of the proposed finite position set simplified predictive control of SynRM.

## V. RESULTS AND DISCUSSION

The validity of the proposed method is evaluated by simulations and experiments.

### A. SIMULATION RESULTS

The simulations are performed to check the proposed method in several scenarios and also compare it with the previous MRAS method. The specification of the simulated motor is listed in Table 1.

The performance of the proposed method is studied in a wide range of speed including the motor and generator modes, i.e., 100%, 66%, 33%, −33%, and -66% nominal speed, and the results are reported in Fig. 4. The results showed that the motor current is fully under control in both d-axis and q-axis directions. The q-axis current is the torque controller component of the current which shows a fast dynamic response. The d-axis current is the flux control component and it is fixed during the test. Six values of the

**TABLE 1. Parameters of SynRM in simulations.**

| Parameter | Description | value |
|---|---|---|
| $P_n$ | nominal Power | 1.5 [kW] |
| $f_n$ | nominal frequency | 50 [Hz] |
| $T_n$ | nominal torque | 10 [Nm] |
| $I_n$ | nominal current | 8.65 [A] |
| $L_d$ | d-axis inductance | 0.12 [mH] |
| $L_q$ | q-axis inductance | 0.034 [mH] |
| $R_s$ | Stator resistance | 2.5 [Ω] |
| $p$ | pole pairs | 2 |

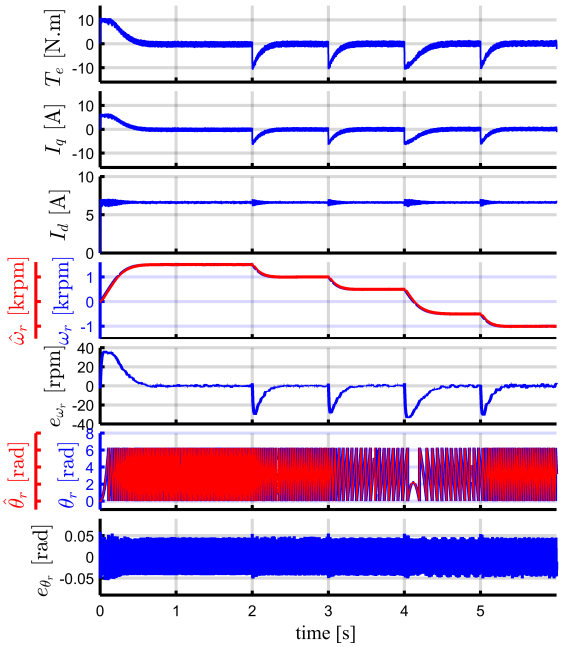


**FIGURE 4. Performance of the proposed method in a wide speed range of motor and generator modes.**

speed reference are examined in this study. It shows that the proposed sensorless predictive control can perform in a wide speed range. The maximum speed reference is +1500 rpm and the minimum is −1000 rpm which examines the performance in both motor and generator modes. It can be seen that the maximum value of the position estimation error was at the designed value and it took place in the zero speed crossing. The position error showed an increase in the dynamic states but the dynamic of tracking back to the minimum value was fast based on the finite position set algorithm. Also, the q-axis current showed a fast dynamic in every speed change due to the production of the deceleration torque. The d-axis current is fixed for all speed references. There was a tiny increase for the ripple of the d-axis current in the dynamic state because of using voltage-based cost function (3). In this method, the direct control of torque and flux or direct control of the current is replaced by the voltage control. Instead, there is no need for tuning the weighting factor for every speed reference.

The low speed performance is also studied in an individual simulation and the results are depicted in Fig. 5. The speed

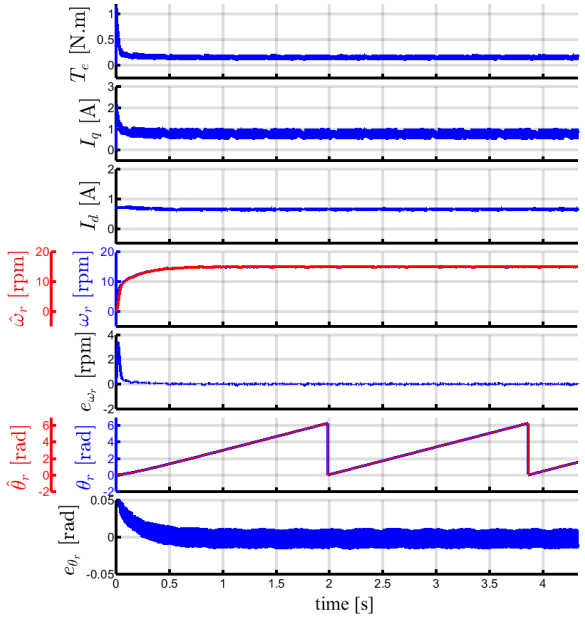


**FIGURE 5. Low speed performance of the proposed method.**

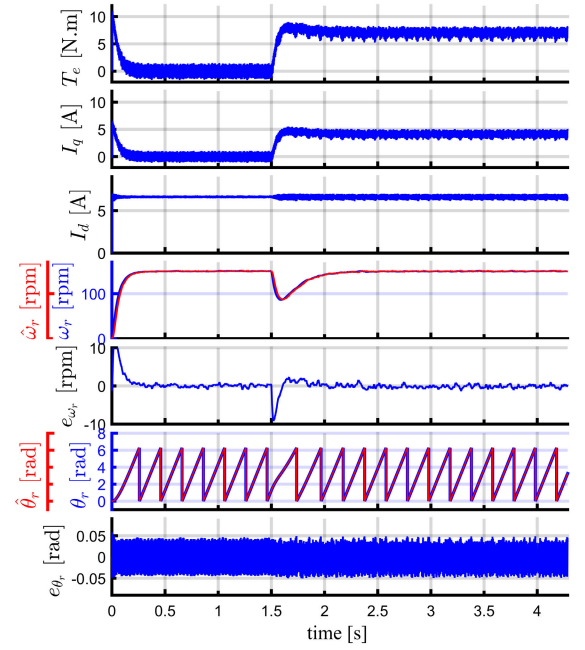


**FIGURE 6. Load disturbance study in low speed condition.**

reference is 1% nominal speed. The maximum of the error of the position is 2.9° which is only 0.3° bigger than the designed value.

The load disturbance is studied in Fig. 6. This scenario is studied during the low speed performance in order to create a very sensitive condition. The result showed that the method was stable during and after the load insertion. The position error is almost equal before and after the load insertion.

In order to evaluate the effect of the contribution of this research, the proposed method is compared to the previous

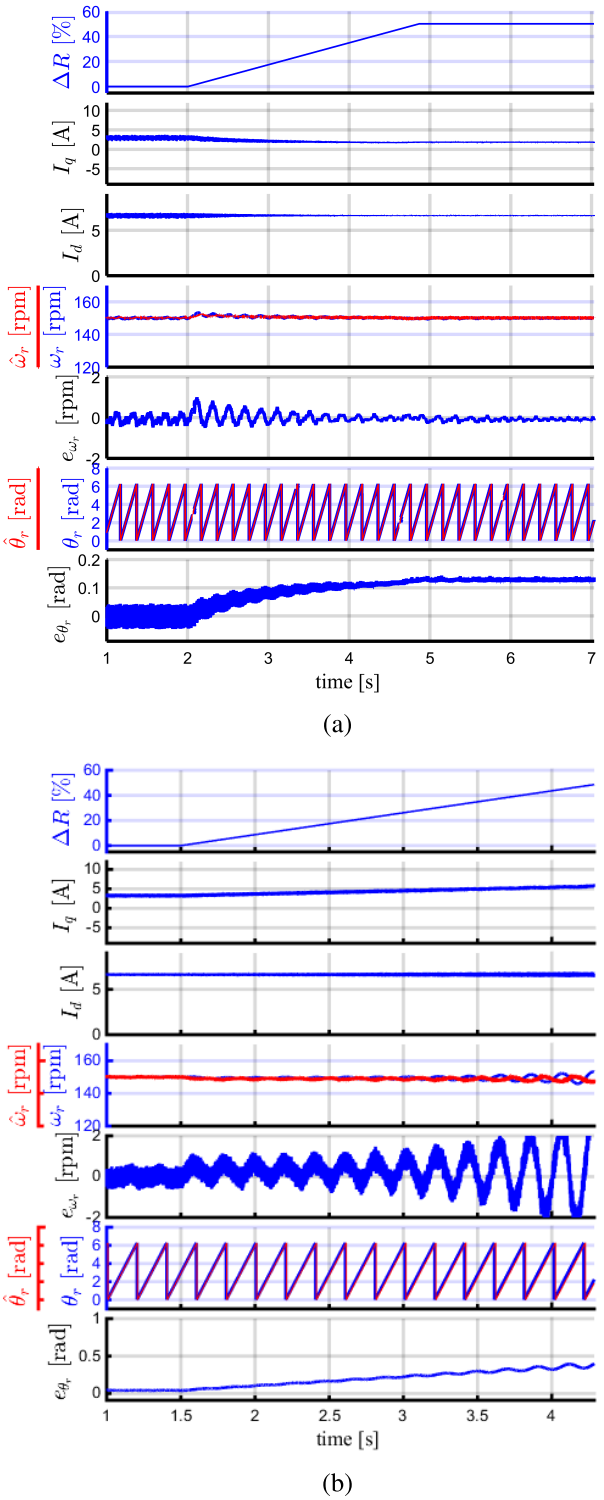


**FIGURE 7.** Robustness study for resistance variation (a) proposed method (b) previous method.

MRAS function [30] and the result is shown in Fig. 7. A resistance mismatch is inserted for both methods and the behaviours are compared. Based on the results, the ripples for the proposed method was 13.7% rated current before the parameter mismatch and it was 9.5% for the previous method and the maximum position error was 0.046 rad for the proposed method and it was 0.04 rad for the previous method which is because of the reduction of the iterations. However, after the stator resistance mismatch, the proposed method was more robust. That is because of the proposed stable error function while the number of iterations is less for the proposed method.

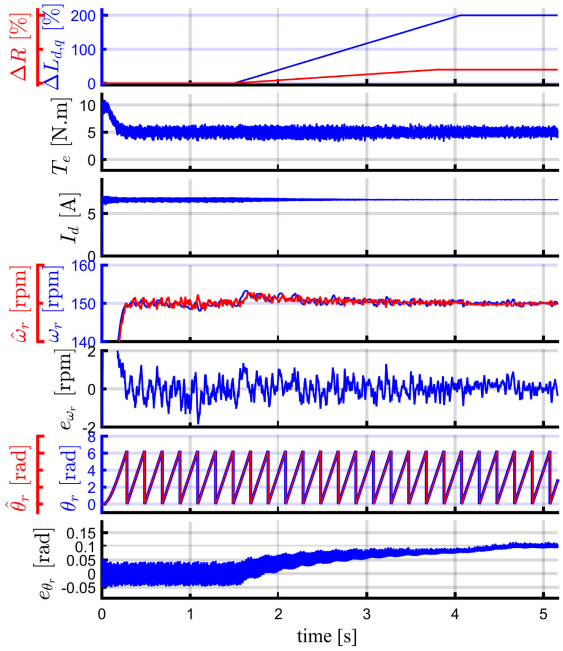


**FIGURE 8.** The behaviour of the proposed scheme in the mismatch of resistance and inductances.

In order to study the effect of the mismatch of all parameters, 40% error for the stator resistance and 200% error for the $L_d$ and $L_q$ are considered for the proposed method and the result is shown in Fig. 8. Note that these parameters are gradually changed in the observer and predictive model, i.e., (5), (10), and (11). It can be seen that the maximum position error is almost equal to that when only the resistance had the mismatch. Thus, the most sensitive parameter is stator resistance. Nevertheless, the results showed that the method was stable when the mismatch error was 200%. Thus, the robustness of the proposed method is concluded.

### B. EXPERIMENTAL RESULTS

The performance of the proposed method for speed estimation has been tested experimentally in this part. To obtain these experimental results, the DSP-TMS320f28335 processor was used as the controller. Because the synchronous reluctance motor was not available in the laboratory for experimental tests, a wound rotor salient pole synchronous machine with open field winding was used instead of it. If the rotor winding is kept open during the experiments, the machine will act based on its reluctance torque. The specifications of the synchronous motor are listed in Table 2. A photograph of the test system is shown in Fig. 9.

**TABLE 2. Parameters of the experimental setup.**

| Parameters of SynRM | | |
|---|---|---|
| Parameter | Description | value |
| $P_n$ | nominal Power | 175 [W] |
| $f_n$ | nominal frequency | 50 [Hz] |
| $T_n$ | nominal torque | 1.1 [Nm] |
| $I_n$ | nominal current | 0.17 [A] |
| $L_d$ | d-axis inductance | 0.39 [mH] |
| $L_q$ | q-axis inductance | 0.01 [mH] |
| $R_s$ | Stator resistance | 4 [Ω] |
| $p$ | pole pairs | 2 |
| Parameters of Inverter | | |
| Parameter | Description | value |
| $I_n$ | nominal Current | 25 [A] |
| $V_n$ | nominal Voltage | 600 [V] |
| Parameters of Processor TMS320F28335 | | |
| Parameter | Description | value |
| $f_p$ | Processing frequency | 150 [MHz] |

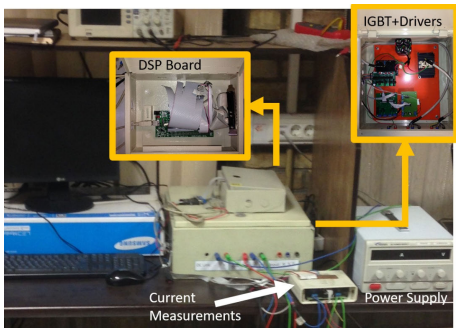


(a)

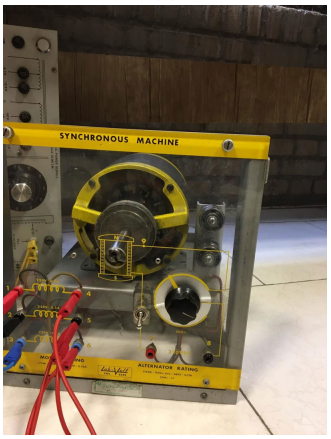


(b)

**FIGURE 9. Photograph of test system (a) control and power systems (b) motor.**

Fig. 10 shows the response of the proposed method in different operating points. In this test, the speed reference is changed by three steps. The speed reference is increased from zero to 100% nominal speed at the startup. Then it is reduced to 66% and finally, it is set to 33%. The mean value of the measured current ripple is 9.18% which is a little bigger than the designed value (5%). The mean value of the position error is 0.066 rad which is smaller than the designed value. Thus, the expected accuracy of the estimation is achieved.

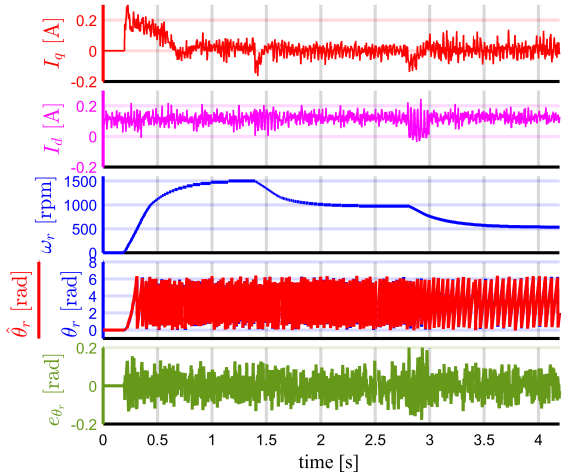


**FIGURE 10. Experimental result of the proposed method.**

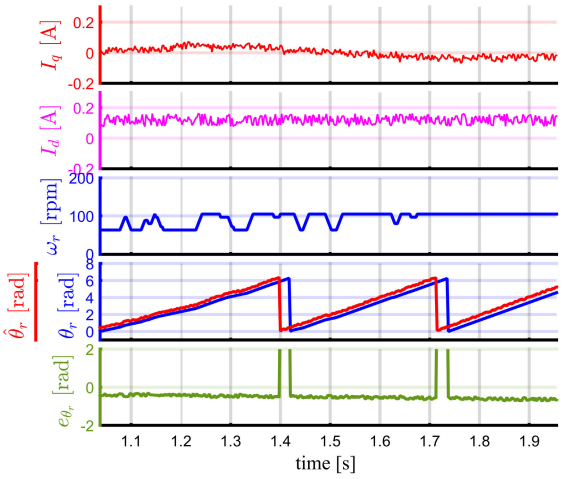


**FIGURE 11. Experimental result of the proposed method at very low speed.**

The experimental performance of the proposed method at the lowest stable speed is reported in Fig. 11. The speed reference is set to 6% nominal speed. It can be seen that there is a stable oscillation in the quadrant component of the current.

## VI. CONCLUSION

The finite position set technique is modified and applied to sensorless predictive control of synchronous reluctance motor. Since there is no rotor winding in this motor, the conventional error function of the MRAS method could not be useful for this method. A stable error function was proposed and applied for the finite position set MRAS technique. Furthermore, the number of iterations has been optimized by considering the sensitivity of the current prediction to the estimated position in this research. In order to further reduction of the repetitive computations, a simplified predictive control was applied in this research. By this method, the number of times that the prediction computation should be repeated is one instead of seven.

The validity of the proposed method is examined by simulation and experiment. The results showed that the error of the estimated position was very close to the designed value during the optimization of the iteration number. Also, the current ripples were achieved as expected based on that optimization. The technique was robust to the resistance and inductance mismatch because of the proposed error function. The comparative results showed that the robustness of the proposed method is improved compared to the previous method. Also, it was concluded that the sensitivity of the method to the resistance was more than that to the inductances. The method could tolerate more than 40% error for the stator resistance and 200% error for the direct and quadratic inductances.

## REFERENCES

[1] S. Taghavi and P. Pillay, "A sizing methodology of the synchronous reluctance motor for traction applications," *IEEE J. Emerg. Sel. Topics Power Electron.*, vol. 2, no. 2, pp. 329–340, Jun. 2014.
[2] T. A. Lipo, "Recent progress in the development in solid-state AC motor drives," *IEEE Trans. Power Electron.*, vol. PEL-3, no. 2, pp. 105–117, Apr. 1988.
[3] L. Cavanini, G. Cimini, G. Ippoliti, and A. Bemporad, "Model predictive control for pre-compensated voltage mode controlled DC–DC converters," *IET Control Theory Appl.*, vol. 11, no. 15, pp. 2514–2520, Oct. 2017.
[4] S. Carpiuc and C. Lazar, "Real-time constrained current control of permanent magnet synchronous machines for automotive applications," *IET Control Theory Appl.*, vol. 9, no. 2, pp. 248–257, Jan. 2015.
[5] A. Morsi, H. S. Abbas, and A. M. Mohamed, "Wind turbine control based on a modified model predictive control scheme for linear parameter-varying systems," *IET Control Theory Appl.*, vol. 11, no. 17, pp. 3056–3068, Nov. 2017.
[6] B. Wang, L. Yang, F. Wu, and D. Chen, "Fuzzy predictive functional control of a class of non-linear systems," *IET Control Theory Appl.*, vol. 13, no. 14, pp. 2281–2288, Sep. 2019.
[7] L. Cavanini, G. Cimini, and G. Ippoliti, "Computationally efficient model predictive control for a class of linear parameter-varying systems," *IET Control Theory Appl.*, vol. 12, no. 10, pp. 1384–1392, Jul. 2018.
[8] S. C. H. Hadla, "Active flux based finite control set model predictive control of synchronous reluctance motor drives," in *Proc. 18th Eur. Conf. Power Electron. Appl. (EPE ECCE Europe)*, Sep. 2016, pp. 1–10.
[9] F. Wang, X. Mei, J. Rodriguez, and R. Kennel, "Model predictive control for electrical drive systems—An overview," *CES Trans. Electr. Mach. Syst.*, vol. 1, no. 3, pp. 219–230, Sep. 2017.
[10] S. Chai and L. Wang, "Finite control set model predictive control of 2LVSI-PMSM using interpolated switching states," in *Proc. Ind. Electron. Soc. Conf. (IECON)*, Oct. 2012, pp. 1799–1804.
[11] C. Xia, T. Liu, T. Shi, and Z. Song, "A simplified finite-control-set model-predictive control for power converters," *IEEE Trans. Ind. Informat.*, vol. 10, no. 2, pp. 991–1002, May 2014.
[12] P. Vas, *Sensorless Vector and Direct Torque Control* (Monographs in Electrical and Electronic Engineering). New York, NY, USA: Oxford Univ. Press, 1998.
[13] A. Aliaskari, B. Zarei, S. A. Davari, F. Wang, and R. M. Kennel, "A modified closed-loop voltage model observer based on adaptive direct flux magnitude estimation in sensorless predictive direct voltage control of an induction motor," *IEEE Trans. Power Electron.*, vol. 35, no. 1, pp. 630–639, Jan. 2020.
[14] S. A. Davari and J. Rodriguez, "Predictive direct voltage control of induction motor with mechanical model consideration for sensorless applications," *IEEE J. Emerg. Sel. Topics Power Electron.*, vol. 6, no. 4, pp. 1990–2000, Dec. 2018.
[15] C. Liu and Y. Luo, "Overview of advanced control strategies for electric machines," *Chin. J. Electr. Eng.*, vol. 3, no. 2, pp. 53–61, 2019.
[16] Y. Zhao, C. Wei, Z. Zhang, and W. Qiao, "A review on position/speed sensorless control for permanent-magnet synchronous machine-based wind energy conversion systems," *IEEE J. Emerg. Sel. Topics Power Electron.*, vol. 1, no. 4, pp. 203–216, Dec. 2013.
[17] Y. Zhao, W. Qiao, and L. Wu, "Improved rotor position and speed estimators for sensorless control of interior permanent-magnet synchronous machines," *IEEE J. Emerg. Sel. Topics Power Electron.*, vol. 2, no. 3, pp. 627–639, Sep. 2014.
[18] Y. Zhao, W. Qiao, and L. Wu, "An adaptive quasi-sliding-mode rotor position observer-based sensorless control for interior permanent magnet synchronous machines," *IEEE Trans. Power Electron.*, vol. 28, no. 12, pp. 5618–5629, Dec. 2013.
[19] A. Yousefi-Talouki, P. Pescetto, G. Pellegrino, and I. Boldea, "Combined active flux and high-frequency injection methods for sensorless direct-flux vector control of synchronous reluctance machines," *IEEE Trans. Power Electron.*, vol. 33, no. 3, pp. 2447–2457, Mar. 2018.
[20] M. Tursini, M. Villani, G. Fabri, S. Paolini, A. Credo, and A. Fioravanti, "Sensorless control of a synchronous reluctance motor by finite elements model results," in *Proc. IEEE Int. Symp. Sensorless Control Electr. Drives (SLED)*, Sep. 2017, pp. 19–24.
[21] S. Nalakath, Y. Sun, M. Preindl, and A. Emadi, "Optimization-based position sensorless finite control set model predictive control for IPMSMs," *IEEE Trans. Power Electron.*, vol. 33, no. 10, pp. 8672–8682, Oct. 2018.
[22] M. F. Elmorshedy, W. Xu, Y. Liu, and M. Dong, "A sensorless finite-set model predictive direct thrust control of a linear induction motor based on MRAS for linear metro," in *Proc. IEEE Int. Electr. Mach. Drives Conf. (IEMDC)*, May 2019, pp. 1336–1341.
[23] F. Wang, S. A. Davari, Z. Chen, Z. Zhang, D. A. Khaburi, J. Rodríeguez, and R. Kennel, "Finite control set model predictive torque control of induction machine with a robust adaptive observer," *IEEE Trans. Ind. Electron.*, vol. 64, no. 4, pp. 2631–2641, Apr. 2017.
[24] M. S. Zaky, "Stability analysis of speed and stator resistance estimators for sensorless induction motor drives," *IEEE Trans. Ind. Electron.*, vol. 59, no. 2, pp. 858–870, Feb. 2012.
[25] F. Wang, X. Mei, H. Dai, S. Yu, and P. He, "Sensorless finite control set predictive current control for an induction machine," in *Proc. IEEE Int. Conf. Inf. Automat.*, Aug. 2015, pp. 3106–3111.
[26] J. Rodas, F. Barrero, M. R. Arahal, C. Martin, and R. Gregor, "Online estimation of rotor variables in predictive current controllers: A case study using five-phase induction machines," *IEEE Trans. Ind. Electron.*, vol. 63, no. 9, pp. 5348–5356, Sep. 2016.
[27] D. Traoré, A. Glumineau, and J. de Leon, "Sensorless induction motor adaptive observer-backstepping controller: Experimental robustness tests on low frequencies benchmark," *IET Control Theory Appl.*, vol. 4, no. 10, pp. 1989–2002, Oct. 2010.
[28] Y. B. Zbede, S. M. Gadoue, and D. J. Atkinson, "Model predictive MRAS estimator for sensorless induction motor drives," *IEEE Trans. Ind. Electron.*, vol. 63, no. 6, pp. 3511–3521, Jun. 2016.
[29] M. Abdelrahem, R. Kennel, C. Hackl, M. Dal, and J. Rodríguez, "Efficient finite-position-set MRAS observer for encoder-less control of DFIGs," in *Proc. IEEE Int. Symp. Predictive Control Electr. Drives Power Electron. (PRECEDE)*, May 2019, pp. 1–6.
[30] M. Abdelrahem, C. M. Hackl, and R. Kennel, "Finite position set-phase locked loop for sensorless control of direct-driven permanent-magnet synchronous generators," *IEEE Trans. Power Electron.*, vol. 33, no. 4, pp. 3097–3105, Apr. 2018.

**BEHNAM NIKMARAM** was born in Tehran, Iran, in 1994. He received the B.Sc. degree from the Islamic Azad University-South Tehran Branch, Tehran, in 2016, and the M.Sc. degree from the Shahid Rajaee Teacher Training University, Tehran, in 2020. He is currently a Research Engineer in the motor control, sensorless drives, and power electronics with the Niroo Research Institute.

**S. ALIREZA DAVARI** (Senior Member, IEEE) was born in Tehran, Iran, in 1981. He received the M.Sc. and Ph.D. degrees from the Iran University of Science and Technology (IUST), Tehran, in 2006 and 2012, respectively. From 2010 to 2011, he left for a sabbatical visit with the Technische Universität München, Germany. From 2013 to 2020, he was with Shahid Rajaee Teacher Training University, as an Assistant Professor, where he has been an Associate Professor, since 2020. His research interests include encoder-less drives, predictive control, power electronics, and renewable energy.

**PEYMAN NADERI** was born in Ahvaz, Iran, in 1975. He received the B.S. degree in electronic engineering in 1998, the M.S. degree in power engineering from Shahid Chamran University of Ahvaz, Iran, in 2001, and the Ph.D. degree in power engineering science from K. N. Toosi University of Technology, Tehran, Iran. He is currently an Associate Professor with Shahid Rajaee Teacher Training University, Tehran. His interests include electrical machine modeling, fault diagnosis, and power system transient.

**CRISTIAN GARCIA** (Member, IEEE) received the M.Sc. and Ph.D. degrees in electronics engineering from Universidad Tecnica Federico Santa Maria (UTFSM), Valparaiso, Chile, in 2013 and 2017, respectively. In 2016, he was a Visiting Ph.D. Student with the Power Electronics Machines and Control (PEMC) Group, University of Nottingham, U.K. From 2017 to 2019, he was with the Engineering Faculty, Universidad Andrés Bello, Santiago, Chile, as an Assistant Professor. Since 2019, he has been with the Engineering Faculty, Universidad de Talca, Curico, Chile, where he is currently an Assistant Professor. His research interests include electric transportation applications, variable-speed drives, matrix converters, and model predictive control of power converters and drives.

**JOSE RODRIGUEZ** (Fellow, IEEE) received the B.E. degree in electrical engineering from the Universidad Técnica Federico Santa Maria, Valparaiso, Chile, in 1977, and the Dr.-Ing. degree in electrical engineering from the University of Erlangen, Erlangen, Germany, in 1985. Since 1977, he has been with the Department of Electronics Engineering, Universidad Técnica Federico Santa Maria, where he was a Full Professor and the President. Since 2015, he has been the President with Universidad Andrés Bello in Santiago, Chile, where he is a Full Professor, since 2019. He has coauthored two books, several book chapters, and more than 400 journal and conference papers. His main research interests include multilevel inverters, new converter topologies, control of power converters, and adjustable-speed drives. He is currently a member of the Chilean Academy of Engineering. He received a number of best paper awards from journals of the IEEE, the National Award of Applied Sciences and Technology from the Government of Chile, in 2014, and the Eugene Mittelmann Award from the Industrial Electronics Society of the IEEE, in 2015.